

The dynamics of strong turbulence at free surfaces. Part 1. Description

By M. BROCCINI¹ AND D. H. PEREGRINE²

¹D.I.Am., Università di Genova, 16145 Genova, Italy

²School of Mathematics, University of Bristol, Bristol BS8 1TW, UK

(Received 24 January 2000 and in revised form 9 July 2001)

A free surface may be deformed by fluid motions; such deformation may lead to surface roughness, breakup, or disintegration. This paper describes the wide range of free-surface deformations that occur when there is turbulence at the surface, and focuses on turbulence in the denser, liquid, medium. This turbulence may be generated at the surface as in breaking water waves, or may reach the surface from other sources such as bed boundary layers or submerged jets. The discussion is structured by consideration of the stabilizing influences of gravity and surface tension against the disrupting effect of the turbulent kinetic energy. This leads to a two-parameter description of the surface behaviour which gives a framework for further experimental and theoretical studies. Much of the discussion is necessarily heuristic, and is often limited by a lack of appropriate experimental observations. It is intended that such experiments be stimulated, to test the value or otherwise of our two-parameter description.

1. General introduction

This study is motivated by a wish to model the spilling breakers that arise at the crests of steep water waves; for example as an ocean wave approaches a beach. The water falling down the front of the wave can be in extremely violent motion with much splashing, see figure 1. Further, the generation and maintenance of this turbulent flow involves strong interactions with gravity. The flow down the front of the wave, from the crest of the wave, drives the forward advance of the breaker. Details of this flow are not understood and such understanding forms one of our major aims. At the start of this study it became clear that, to make an effective model, better general understanding of strongly turbulent flows at a free surface is needed. By ‘strong’ turbulence we mean turbulence which is sufficiently energetic that it causes the free surface to be strongly distorted. Such distortion may range across the generation of surface waves, projections, cusps and dimples to surface breakup with creation of drops, bubbles and fully mixed two-phase flows. Attention is restricted to liquid–gas interfaces, and to turbulent flow in the liquid, generally neglecting the dynamic effects of the gas.

Our aim is that eventually we might usefully model unsteady breakers. We draw attention to two aspects of such flows where we lack any detailed models. The source of turbulence in a breaker is at or close to the free surface, yet we are not able to fully identify the turbulent production mechanisms. Deep water breaking is usually relatively brief with the region of active turbulence generation often being left behind as the wave crests advance. The evolution, and decay of generation of



FIGURE 1. Photograph of a spilling breaker propagating toward the left. This is an example where much of the visible 'white water' may be an interpenetrating mixture of both air and water.

such turbulence when it is not on the front of a wave crest needs greater insight for successful modelling. We only make slight progress towards a full solution of these problems and much of our discussion relates to steady mean flows. An example of such a steady flow is given in figure 2, which shows a small hydraulic jump in a laboratory flume. The flow approaching from the right-hand side is about 4 cm deep and due to the substantial convergence of the flow as it passes over the weir it has a low level of turbulent velocity perturbations, probably less than 10% of the mean flow velocity. The incoming water surface appears smooth and may be contrasted with the convoluted surface of the breaker forming the hydraulic jump. In addition note that only a few air bubbles are being entrained. Further properties of the breaker are illustrated by red dye that was added from a tube that is visible as an oblique bright line at the top of the photograph. The dye was added as occasional drops about once every two seconds. The original aim was to see the extent of flow down the surface of the breaker. However, as each drop entered the water the result was dramatic. In a small fraction of a second the dye spread to most of the turbulent region in which it is visible as a darker shade in the photograph. In essence this shows that the turbulent velocity fluctuations are of the same magnitude as the incoming mean velocity. Further discussion of this flow may be found in Peregrine & Svendsen (1978), and further photographs for a slightly weaker breaker with no air entrainment are shown in figure 5. General points to note here are

- (i) the high level of turbulence originates from the free surface—its generation mechanism is not entirely clear and is a major target of our studies;
- (ii) in this paper we concentrate our discussion on the region close to the free surface where the presence of each phase, air and water, is intermittent. This precludes the use of some useful concepts such as Fourier representations;

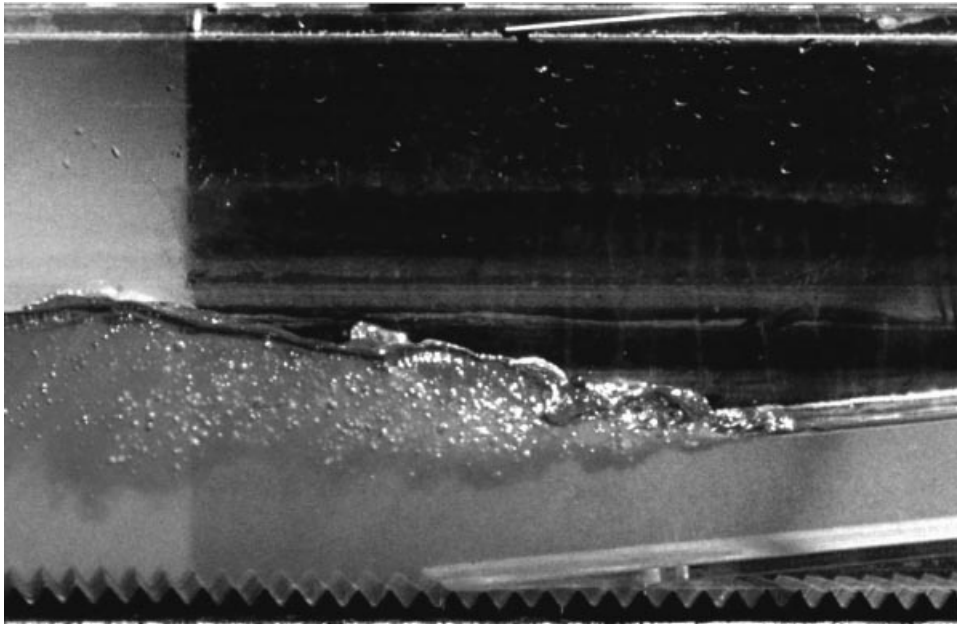


FIGURE 2. Photograph of a hydraulic jump on a flow entering from the right. The volume of turbulence originating at the free surface is marked by dye.

(iii) as figures 1 and 2 illustrate, the free surface can respond to turbulence in differing ways.

There are numerous studies of turbulent flow at a free surface. Those which seek to model the turbulence fall into three categories:

(a) approximations to large portions of the turbulent flow. Of these the discontinuity model for a bore or hydraulic jump is well known, and the ‘roller’ model of Schäffer, Madsen & Deigaard (1995) is becoming popular;

(b) averages over the turbulent fluctuations;

(c) direct simulation of details of the turbulent flow.

We are mainly concerned with the second of these categories where Reynolds-averaged equations require closures to be chosen for averages over products of the primary variables. In particular, we address the problem of averaging over a non-smooth, or disconnected free surface in Part 2 (Brocchini & Peregrine 2001). However, this study also provides useful guidance for the simpler type of modelling. An important preliminary is the identification of the various flow regimes that can occur, and is the focus of this paper.

The most interesting flows are those, as in figure 1, which are strongly nonlinear and splashing, but even the much smoother flows occurring in small ‘micro-scale’ breakers that are restrained by surface tension, as in figure 5, also require attention. Experimental work on disturbed air–water interfaces is mainly concerned with two fundamental aspects. On the one hand the mechanism of generation and the dynamics of small-scale features of the free surface are studied. These may be both the ripples at the front of gentle spilling breakers (e.g. Duncan & Dimas 1996; Duncan *et al.* 1999) and the water columns, ejections, drops and bubbles induced by turbulent water structures impinging on the free surface (e.g. Davies & Driscoll 1974; Clift, Grace & Weber 1978; Volkart 1980; Rein 1998). A few experiments are also aimed at a quantitative prediction in terms of synthetic parameters of the onset of steep, capillary

ripples which characterize micro-breakers of different types (e.g. Lin & Rockwell 1995; Walker, Chen & Willmarth 1995). The second important object of experimental analysis is the role played by water surface features like those typical of micro-breakers in air–water gas and mass exchange. Recent works analyse the possible regimes that govern aeration rates like turbulent transport and bubble-dominated transport (Boettcher, Fineberg & Lathrop 2000) and parametrize the intensity of air–water gas transfer in terms of global parameters like the fractional area coverage of micro-scale breaking waves (e.g. Zappa, Asher & Jessup 2001).

There is no good description of free-surface boundary conditions for a strongly turbulent flow. Almost all modelling to date has taken linearized boundary conditions (e.g. Walker 1997) and/or inappropriate turbulent averages of the surface, or else has made approximations for large portions of the turbulent flow field at once. Aspects that are omitted in any linearization are the mass and momentum flows associated with the fluctuations of the free surface. For the more organized motion that occurs in water waves this mass flow is relatively well known and described as Stokes drift. In an Eulerian description this is normally thought of as the mass flow associated with the fluctuations of the free surface. Hasselmann (1971) is the only paper we are aware of that describes both the Stokes drift and its equivalent for turbulent flows for the case of a smooth surface. Little notice seems to have been taken of that paper and in Part 2 we make equivalent, but more general, derivations of these results due to surface fluctuations. Once a free surface is convoluted or disconnected, then the flow close to the surface can reasonably be described as a two-phase flow, and Chen *et al.* (1996) describe the evolving free surface from a Rayleigh–Taylor instability in this way, but take a mixed region rather than treating it as a boundary. The work of Hong & Walker (2000), who use the level-set method of dealing with the two-phase nature of the flow, is an interesting exception to the above comments: it shows how induced flow at a free surface can have a major effect on the flow of a turbulent jet. Also Hodges & Street (1999) derives a large-eddy-simulation technique for finite-amplitude free surface displacements.

There are wide differences in the free surface behaviour at different length scales since surface tension is important for small length scales and gravity for large length scales (e.g. Davies 1972). The results required from turbulent free-surface flow hydrodynamics also differ widely. Application to forces on structures may only depend on the largest scales whereas heat or mass transfer between gas and liquid may depend strongly on the smaller scales even in a large-scale flow. The wide variety of free-surface flows and their different scales of motion are likely to need different closures for averaging over the turbulence. First we note some general aspects of the problem.

Although this study is motivated by the spilling breakers that occur as water waves advance towards a beach, there is a wide range of other flows where turbulence strongly deforms a free surface. Wind-generated breakers are likely to be very similar to those generated on beaches. Yet, although there are differences, especially due to the shear in the water, there appears to have been no detailed study of them. Theoretical work on waves with shear, e.g. Teles da Silva & Peregrine (1988) that shows a strong effect of vorticity on the height of the limiting waves, has yet to be effectively linked with wind wave breaking, though Banner & Tian (1998) have used Dold & Peregrine's (1986) boundary-integral method to compute how two-dimensional waves on a shear approach breaking. Douglas & Weggel (1988) describe some qualitative laboratory experiments of the effect of wind on waves breaking on a beach, confirming that there is a strong effect.

On the other hand the gas–liquid interactions in more confined circumstances such as co-current stratified two-phase flow in a pipe shows very different behaviour. Here the surface can be almost perfectly smooth between turbulent slugs which involve a highly turbulent gas–liquid mixture (e.g. Maron *et al.* 1991). We suspect that the importance of the gas phase in the flow dynamics increases as the gas becomes more confined and where the gas also plays a part in driving the liquid (see Thorpe 1995 for a good review on the dynamical processes of transfer at the sea surface). However, to keep the discussion and analysis relatively simple we include little consideration of the gas phase here, although much of our work might be extended to include its influence, and we do use ideas from the study of two-phase flow.

It is useful to note the differing character of the numerous instances of strong turbulence at a free surface. Wave breaking is an example where the turbulence is generated at the free surface, but equally common are examples where turbulence reaches a free surface from below, or turbulent flow emerges from an enclosed or partly enclosed region. Examples of the former are flows down steep rivers or artificial spillways where turbulence generated at the bed can be strong enough when it reaches the surface to cause spray and result in ‘self-aerating’ flows. The flows down dam spillways have received detailed experimental study, for example see Bremen & Hager (1989), and Chanson (1993, 1995, 1996). Similarly there is descriptive documentation of the surface features of turbulence in rivers, e.g. Nezu & Nagakawa (1993).

Among reviews of turbulence at a free surface, and closely related topics such as vortical flows near a free surface, are those of Sarpkaya (1996), Tsai & Yue (1996) and Melville (1996), all in the same volume of *Annual Reviews of Fluid Dynamics*, yet with reference lists that are almost entirely independent of each other!

More basic studies by Komori, Murakami & Ueda (1989) and Rashidi, Hetsroni & Bannerjee (1992) are on the relationship between existing turbulent structures in the flow beneath the free surface and the dynamics of the surface itself. In addition there is a body of literature on heat and mass transfer at the air–sea interface, see for example Wilhelms & Gulliver (1991). These studies have generated the concept of a ‘surface skin’, which when broken by large eddies or by breaking water waves leads to surface ‘renewal’ and enhancement of air–water transfers.

Examples of numerical studies of turbulence at a free surface are the direct numerical simulations by Handler *et al.* (1993), Borue, Orszag & Staroselsky (1995), Pan & Banerjee (1995) and Tsai (1998). It is found that the effect of a linearized free surface on turbulence has some similarities to that of a rigid boundary but there are differences. These directly affect the velocity field, e.g. vortex lines can attach to a fluid–fluid interface, whereas they cannot attach at a no-slip boundary on a rigid surface which is at rest or in uniform motion; hence Walker’s (1997) discussion of the ‘surface current’.

Shen *et al.* (1999) also simulate turbulence with linearized boundary conditions, and discuss the relatively slight differences from no-slip boundaries. More relevant is their discussion of two ‘surface layers’, first identified by Hunt & Graham (1978) for a co-moving rigid boundary. One is the free-surface viscous boundary layer; as one can expect from consideration of other boundary layers at the free surface, its thickness scales with the square root of the local Reynolds number. The other is a thicker ‘blockage’ layer due to the normal relative velocity components being strongly constrained at the free surface. It scales with the typical turbulent length scale, and through this layer the turbulent fluctuations become predominantly parallel to the free surface. We mention these layers since we also discuss a surface layer which differs from both of these. It is with regret that we also note that discussion of the

viscous boundary layer has often simply used the term 'surface layer'. Here we consider turbulence sufficiently strong that the viscous boundary layer is generally of negligible thickness compared with the surface distortions. Also, the blockage layer can be much reduced, or entirely negligible when the constraints of gravity and surface tension are insufficient to restrict vertical velocity fluctuations near the mean free surface.

In this paper, we describe the varied character of a free surface distorted by turbulence. This depends on the strength of the turbulence and its length scale. The main portion of this paper is a phenomenological introduction to the various types of flow regimes that can be found. There is a need to introduce terminology to describe these differing classes of surface disturbance. Some of the regimes are scarcely recognized in the literature and deserve more study; hence §2 gives a brief overview of the subject. Such study needs to be quantified and as such clearly needs a description of the disturbing turbulence as well as the restraining influences of gravity and surface tension. These influences can usefully be described in terms of dimensionless Froude and Weber numbers; however, since the majority of applications relate to a water–air interface in normal terrestrial gravity, much of our discussion relating to these two parameters is in dimensional terms. The following discussion is then based on particular regions of the parameter space. It aims to go a little beyond the results obtainable by simple consideration of dimensionless numbers in assessing the boundary between different regimes. However, it is mainly descriptive, often based on much personal observation. In some circumstances other features such as surface-active agents and air motions are also important but we generally ignore such complications. It becomes clear that even when suitable averaged boundary conditions are found the particular closures needed are likely to vary with the flow regime.

Part 2 (Brocchini & Peregrine 2001) is a more formal and mathematical account of the flow conditions at a strongly distorted, and possibly disconnected, free surface. Boundary conditions appropriate for use with averaged equations in the body of the water are obtained by integrating across the two-phase surface layer. Preliminary discussions on closure are given for two simplified cases in order to stimulate further experimental and theoretical studies. The paper concludes by considering the spilling breaker and the initiation of turbulence at its forward limit. This is the forward limit of the masses of water tumbling down the front of a spilling breaker where they fall onto the smooth incoming water at the foot of the breaker causing intense generation of turbulence.

Part 3 (Brocchini & Peregrine 2002) continues with the original problem of a spilling breaker. It is mainly concerned with an extension of the model of Madsen & Svendsen (1982) and Svendsen & Madsen (1984) who followed Peregrine & Svendsen's (1978) observation that the layer of turbulence generated by a spilling breaker is relatively thin and developed a thin-layer model to add to the shallow-water wave equations.

Further studies should include a range of closure hypotheses for differing flow regimes, more experimental attention to the concepts developed, and wider applications.

2. General description of disturbed free surfaces

From the wide range of examples of surfaces disturbed by turbulence it is useful to concentrate on two types of flow. One is that of a spilling breaker, and its stationary counterpart the hydraulic jump, and secondly the surfaces disturbed by pre-existing turbulence as from a jet or wake. In both cases the overall flow is steady or quasi-steady with an evolution in turbulence properties from its inception, or

its encounter with a smooth free surface, to its eventual decay in a downstream direction. This evolution is common but not universal. For example, in spillway flows there is a continual input of turbulent energy from the bed and gravity. At inflow the flow's surface suffers little disturbance but turbulence developing from the bed downstream leads to vigorous interactions with the surface. In all cases, many examples of strong interaction between turbulence and a free surface show a whole range of conditions between a quiescent surface, where simple linearized boundary conditions are adequate, to strongly splashing flows which clearly need a different approach.

We commence with the least energetic turbulence, and move to stronger more energetic flows. A weakly deformed free surface can demonstrate three different features:

(a) deformation that is simply a 'passive' response to the turbulent fluctuations of pressure;

(b) water waves;

(c) flows which essentially involve non-uniform vorticity and the free surface.

The first type of response is illustrated well by the surface depression that occurs above the cores of vertically oriented vortices. The case of a Rankine vortex is often used as an elementary example, Lamb (1932, §27). These fluctuations in the free surface can be seen even when the surface is very nearly flat by judicious viewing of objects reflected in the free surface—a relatively neglected method of quantitative observation. As turbulence gets stronger they simply become more evident. In particular, the thin cores of near vertical vortices may give dramatic lowering of the free-surface and lead to some air entrainment. See figure 3 where such vortex 'dimples' and other passive and active free-surface features may be seen. This type of passive free-surface behaviour seems unlikely to have important dynamical consequences other than those inferred from linearized boundary conditions even for moderate slopes, but see below.

Water waves are the typical motion of a free surface. They are usually very well described by irrotational flow and hence might not be considered as part of a turbulent flow. However, note that at the margin of any turbulent flow irrotational fluctuating velocities are induced: at and near a free surface their character may be changed due to the influence of the surface, with wave generation occurring. Also water waves are a potent source of turbulence when they break. Thus water waves and turbulence are intimately related.

Water wave generation by weak turbulence requires a reasonable match of length and time scales between the turbulent motion and free waves, as in Phillips' (1957) resonant interaction theory for water wave generation by wind. This has been extended in Teixeira & Belcher (2000) to generation of waves by subsurface turbulence. Even for this simpler case where linearized boundary conditions can be expected to be valid, those authors comment on the difficulties of finding models for the time and space variation of the pressure. As is well known, free water waves have a minimum phase velocity due to the balance between gravity and surface tension; on water this is about 0.23 m s^{-1} for a wavelength of 17 mm. This indicates a lower bound on the translation velocities of turbulent eddies at which such eddies generate waves. For larger velocities, as was seen at the time the photograph in figure 3 was taken, the erupting nature of the boundary of the turbulent region behaves like a wavemaker around each moving eddy. The resulting waves spread out, as from any other brief localized disturbance. In particular the group of moderately steep waves close to the centre of figure 3 are freshly generated by such an eddying motion.



FIGURE 3. Flow of the River Wye over submerged rocks. Flow is down the picture, which shows an area of roughly $6\text{ m} \times 3\text{ m}$. Each rock is probably about 30 cm in size. The stronger turbulence in the wake of each rock disturbs the surface, showing many of the surface features of weak turbulence. Waves generated by the largest, billowing, turbulent eddies roughly outline the wake. Within the wake dimples and other irregular features give an indication of smaller scale turbulent features.

The converse reaction, of waves incident on moderate strength turbulence, typically leads to dissipation of wave energy, as may be seen from the relatively calm conditions on a ship's wake in an otherwise rough sea. Peregrine (1976) reviews the topic, and more can be found in Boyev (1971) and Ölmez & Milgram (1992). The main overall result is that incident surface waves are damped, strongly so if their wavelength is similar to, or less than, the dominant length scale of the turbulence. For dissipation on a turbulent current see Simons, Grass & Kyriacou (1988) and references therein.

Free-surface features that involve non-uniform vorticity fall into two somewhat overlapping categories. Some are just stronger versions of the 'passive' displacements of the free surface. Others are related to 'separation' of streamlines from the free surface. Separation at a free surface differs somewhat from the corresponding separation at a rigid surface. As an example of this we note the steady flow around a bubble. It may not separate at high Reynolds numbers but can separate at 'intermediate' Reynolds numbers. Blanco & Magnaudet (1995) give details of this type of behaviour by considering ellipsoidal bubbles of differing aspect ratios. However, there are many other facets to this problem, not least the series of flows that can be found commencing at its weakest with the Reynolds ridge (Reynolds 1881; McCutchen 1970). This is associated with a thin layer of separation close to the surface, and as the strength of the flow is increased the Reynolds ridge enters the capillary/gravity regime, with wave generation, and breaking can occur. If the flow's strength and length scale become larger still the separation line becomes a strong depression, sometimes called a 'scar'. Note that the Reynolds ridge usually occurs when there is some surface-active material being swept along the surface. There is another range of surface behaviour depending on the amount of surface 'contamination' which at its most extreme leads to a layer of foam. This is not discussed further here.

'Scars' can be a common feature where turbulence disturbs an almost flat surface. One of the first references to 'scarified' water surfaces can be found in Michels & Lovely (1953). Scars are cusp- or corner-like indentations of the water surface. A scar is most often generated at the edge of a rising burst where the surface dips downwards. Hence a scar can also be defined as a line on the free-surface where fluid is entrained downward from the surface. More recently 'scars' have been discussed as a manifestation of the interaction of patches of vortical flow with a free surface (e.g. Lugt & Ohring 1992; Sarpkaya 1996). A second question concerns the typical width of the scars. This is much smaller than the length scale of the vorticity patch. Hence, in the following analysis we need to be aware that the length scale of the eddies impinging on the water surface may be very much larger than significant small-scale features (indentations, scars, humps, etc.) occurring on the surface itself, e.g. see figure 2 where all the surface features have length scales much smaller than that of the billowing eddies of the wake from a rock, except for the crest length of the waves generated.

Whether we consider passive, wavy or vortical free surface structures, they all develop features like wave breaking as the strength of turbulence is increased. Breaking waves are familiar. Mechanisms concerning other common features are less known: e.g. generation and breakdown of vertical vortices ('bath tub vortex'), breaking and/or folding above horizontal vortices near the free surface and splashing of the free surface.

3. Terminology and quantification

The major influence of turbulence on the free surface comes from the motions of moderately coherent and discrete volumes of fluid that move upward to the surface,

perhaps through it, sometimes falling back on it, or moving parallel to it and hence disturbing it. It is convenient to have a name for such coherent volumes: we call them ‘blobs’. This word conveys the behaviour of the liquid better than the term ‘eddy’ used with single-phase turbulent flow. One way of considering these blobs is to note that they form the boundary of the turbulence, and thus might be represented by the major ‘billows’ at the edge of an active turbulent region. To quantify these blobs we suppose that they have a typical length scale, L , and overall velocity q , with a representative kinetic energy density per unit mass $k = \frac{1}{2}q^2$. The length L may often correspond to the most energetic turbulent scales, so that k has its usual definition as the average $k = \frac{1}{2}\langle u_i u_i \rangle$ where u_i is the turbulent fluctuation velocity. Whatever choice is made for L this is a reasonable choice for the velocity scale. If, as is more appropriate, L is chosen as the length scale of dominant surface features, it represents the result of an interaction between turbulence and the surface effects of gravity and surface tension. Although the direction of motion relative to the free surface strongly affects the surface features, for the present purposes we use a simple scalar velocity parameter, q , since flow direction can vary substantially from blob to blob. We suppose that L and q are independent parameters.

There are also other features to be borne in mind, such as smaller scale features, as seen in figure 2, the downwelling lines of scars around blobs, which have much shorter transverse length scales, and the more point-like depressions terminating strong vortices. In addition, when turbulence disrupts a surface typical length scales fall rapidly as surface-tension-dominated drops and bubbles form. However, we are concerned with the motions that lead to such breakup. Sometimes these are as small in scale as typical drops or bubbles, but are often very much larger.

To chart our discussion of the water surface we consider the two stabilizing factors of gravity and surface tension. We give less attention to the liquid’s viscosity since turbulence is essentially a high Reynolds number phenomenon. Viscosity probably plays a role in maintaining the integrity of the surface for small-scale turbulence. We suggest, from consideration of mixing layers and of inhomogeneous flows such as buoyant plumes, that we are unlikely to have turbulence for Reynolds numbers $Re = qL/\nu < 100$. The brief overview below introduces a more detailed discussion in the following sections (see also Brocchini 1996).

For gravity, g , we compare the corresponding specific energy densities, gL and $\frac{1}{2}q^2$. This leads to a turbulent Froude number $Fr = q/(2gL)^{1/2}$. For low Froude number ($\frac{1}{2}q^2 \ll gL$) and if the turbulence has insufficient energy to disturb the surface, the stabilizing effect of gravity is dominant, leading to a nearly flat surface. This is not the whole story since there is also the shorter length scale of around $q^2/2g$ for which surface displacements may be stronger. At high Froude numbers, $\frac{1}{2}q^2 \gg gL$, the average excursions of the free surface may be expected to be $O(q^2/2g)$, and extreme excursions much greater. The surface is then not restrained by gravity. It is for $Fr \sim O(1)$ that the most varied behaviour can be expected with an interplay between gravity and turbulence with the randomness of turbulence and the structure of waves giving breakers of various sorts.

For surface tension, T , which is a surface energy density, division by density, ρ , gives a specific surface energy, $S = T/\rho$, so we need to compare it with some volume of the liquid and hence we use the representative depth, L , of the turbulent flow or blob. This gives a comparison between $\frac{1}{2}q^2L$ and S , leading to a Weber number $We = q^2L/2S$. As for the Froude number, a low Weber number, $We \ll 1$ implies little or no disturbance to the surface. A high Weber number indicates that the surface

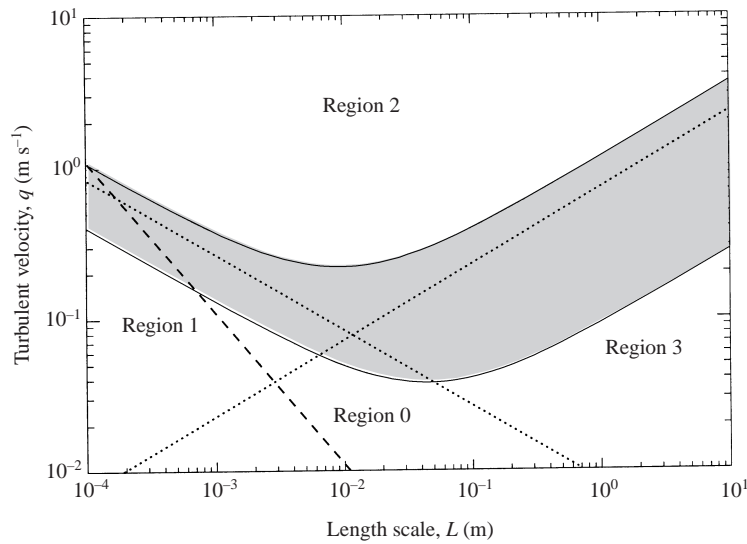


FIGURE 4. Diagram of the (L, q) -plane for water. The shaded area represents the region of marginal breaking and has been obtained by using the two estimated values for both the critical Weber number $[(\pi - 2)/5 < We_c < \pi/4]$ and the critical Froude number $[(5/2 - \pi/2)/250 < Fr_c < \pi/24]$ obtained from equations (3.1) and (3.2). The two straight dotted lines represent a simplified division of the plane for purposes of discussion. The dashed line represents $Re = 100$.

could disintegrate into drops, hence reducing the length scale, and $We \sim O(1)$ leads to surface features that might involve wave-like behaviour.

However, both gravity and surface tension act at a liquid surface so the surface behaviour depends on both Fr and We . Thus the value of both parameters must be considered. We discuss their effect by seeking to delineate a critical region of parameter space between quiescent surfaces and surfaces that break up completely. We illustrate this with a length–velocity diagram in figure 4 where the (L, q) -plane, with logarithmic scales, is shown for water rather than a (Fr, We) -plane. If this critical dividing region were simply defined by specific critical Froude and Weber numbers, this plane would be divided by lines

$$q = \sqrt{2Fr_c gL} \quad \text{and} \quad q = \sqrt{2We_c S/L}$$

where the subscript c denotes a critical value. Such lines are represented by the two straight dotted lines in figure 4. These divide the (L, q) -plane into four regions labelled 0 to 3: each of these regions is discussed below. In addition we find it useful to consider the development, in space or time, of a turbulent surface flow as being represented by a trajectory through the parameter space to describe the growth or decay of turbulence in a specific flow. In this same parameter space we identify the line $Re = 100$: below and to the left of this line viscosity has a dominating effect on the evolution of any turbulence that might be generated.

There is a substantial range of variation between a surface that is no longer smooth because of a turbulent flow and one that is broken up by a turbulent flow, so despite our dividing lines, no precise critical values for Fr and We can be determined. We attempt to show this range in figure 4 by shading the relevant area. The relationship between turbulent kinetic energy and surface state seems to be unexplored. We have found no guidance in the literature and describe below how we have estimated upper

and lower bounds on this transition. It is near these upper and lower bounds for the transition region where we look for critical values.

For an upper critical value our approach is to compare the turbulent kinetic energy density per unit volume of a blob that can disturb the surface with the energy of a surface disturbance per unit surface area. Thus we need to (i) specify a surface deformation, (ii) make a suitable surface average of the change in surface energy compared with the undisturbed horizontal surface and then (iii) decide what depth of liquid below the surface is relevant to the surface dynamics for that deformation. As we indicate, surface features differ depending on the length scales L involved, and also on their spatial frequency. In the discussion below we have made a number of specific choices. Since there are no available experimental data, these are just guesses based on experience from visual observations of various flows.

The upper bound of the transition zone is where the surface is just broken up. We represent this by considering a blob that is just able to generate a spherical drop that just touches the surface when it has lost any overall motion. Each drop of radius R has potential energy $\frac{4}{3}\pi R^3 g R + 4\pi R^2 S$ where we take liquid density to be unity. Now for averaging let us suppose there is one such drop in each square of side $4R$, giving an energy per unit area of $\frac{1}{12}\pi g R^2 + \frac{1}{4}\pi S$. Then if we choose the representative turbulent length L to be $2R$ or half the length of our surface structure, we compare the surface energy to $\frac{1}{2}q^2 L$. This leads to an estimate for the upper bound of the transition zone of

$$q^2 \approx \frac{\pi}{24}gL + \frac{\pi S}{2L} = 0.13gL + 1.57\frac{S}{L}. \quad (3.1)$$

A model surface for a lower bound is less obvious. Surface diffusion studies show that the first indication of turbulence ‘breaking’ the surface can be represented by the creation of fresh surface by the breaking of a surface skin. This could be at, or near, molecular level, but perhaps is better described by the type of continuum surface model Shikhmurzaev (1997, 1998) has introduced. We are primarily looking at dynamic effects, and have already noted the existence of shorter relevant length scales when gravity is dominant. The least disturbance that gives a discontinuity of the surface gradient appears to be converging downwelling motions with the general character of the cusp solution described by Jeong & Moffatt (1992) for Stokes flow. To simplify analysis we consider a linear downwelling feature bounded by two, convex-upward quarter-circles of radius r . Again we do not include any kinetic energy, this time supposing the motions to be part of the turbulence. Using the fact that the centre of mass of a semicircle is $4r/3\pi$ from its bounding diameter, the potential energy per unit length of such a depression is

$$\left(\frac{5}{3} - \frac{1}{2}\pi\right)gr^3 + (\pi - 2)Sr.$$

The depressions need not be especially frequent for them to be important for heat and mass transfer and for vorticity generation, so we suppose that their spacing is $10r$, and again take half this value for the turbulence depth: $L = 5r$. This results in the lower bound of the transition region being

$$q^2 \approx \left(\frac{5}{3} - \frac{\pi}{2}\right)\frac{gL}{125} + \frac{(\pi - 2)S}{5L} = 7.7 \times 10^{-4}gL + 0.22\frac{S}{L}. \quad (3.2)$$

These curves, (3.1) and (3.2), are used to delineate the transition zone in figure 4. It is interesting to contrast these two curves with other cases where we do have information about limiting free-surface shape: that is the organized motion of surface waves on deep water. Solutions of limiting steepness have been found for both

Type of wave	$(aK)_{\max}$	Specific surface energy density	Source
2D propagating (gravity)	0.44	$0.072gK^{-2}$	Cokelet (1977)
3D short crested (gravity)	0.77	$0.088gK^{-2}$	Roberts (1983)
2D standing (gravity)	0.62	$0.077gK^{-2}$	Mercer & Roberts (1992)
2D propagating (capillary)	2.29	$1.90S$	Crapper (1957); Hogan (1979)

TABLE 1. Maximum energy (kinetic plus potential) per unit area for limiting waves. Here g represents the acceleration due to gravity and K the wavenumber.

standing and travelling waves when just gravity acts, and for pure capillary travelling waves. The specific energy density per unit area of these waves is given in table 1. The corresponding depth L , for comparison with the energy per unit volume, is chosen as $L = \pi/K$, i.e. half a wavelength, as in the above example with blobs/drops. If we equate these with $\frac{1}{2}q^2L$ we get for the limiting gravity wave with least energy $q^2 = 0.014gL$. This can be compared with the upper and lower bound gravity terms of (3.1) and (3.2): $0.13gL$ and $0.00077gL$. As we might expect it fits midway between them.

A similar calculation for the maximum travelling capillary wave gives $q^2 = 1.9S/L$ which when compared with surface tension terms $0.23S/L$ and $1.6S/L$ is a little above our chosen upper bound. This seems reasonable since these waves are regular and overhanging whereas turbulence is irregular. We know of no study of extreme standing capillary waves, and leave this topic noting the lack of experimental observations and data in this area.

We observe that if instead of q we consider c , the phase velocity c of linearized gravity–capillary waves on the surface of wavelength $2L = 2\pi/K$ then

$$c^2 = g/K + SK = 0.32gL + 3.1S/L.$$

If this curve is plotted in the parameter plane it lies above our upper bound, (3.1), for the transition region, and is higher than the above energy estimates. This is reassuring since if water velocities in a wave are as high as the wave’s phase velocity then it tends to be breaking.

4. Weak turbulence

When both the Froude number and the Weber number of the turbulence are small, that is region 0 of figure 4, there is little or no surface disturbance, a state which corresponds to the rigid-lid free-slip studies of free-surface turbulence. Numerous important studies have been made on the interaction between turbulence and such a free surface. Recent ones include Gibson & Rodi (1989), Rashidi *et al.* (1992), Handler *et al.* (1993), Borue *et al.* (1995), Walker *et al.* (1995), Walker, Leighton & Garzanos (1996) and Shen *et al.* (1999).

This is perhaps a good point at which to draw attention to the very simple representation of the turbulence we are using for purposes of discussion. Single length and velocity scales are inadequate to represent the multitude of length, time and velocity scales that occur in a turbulent flow. For example, even in a weak turbulent flow there is likely to be some fraction of the disturbances that has time and length scales matching those satisfying the linear surface wave dispersion relation. Indeed, it seems likely that an analysis similar to that of Phillips (1957) for describing

the generation of waves by pressure fluctuations due to wind may be more relevant to the generation of waves by turbulence on the liquid side of the free surface. Teixeira & Belcher (2000) have made some progress in considering such wave generation.

If waves exist on the water surface then weak turbulence with a greater length scale than the waves has an effect on their propagation. This can be significant in its effect if the resulting wave refraction leads to wave focusing.

The free-surface behaviour in this quadrant of the (L, q) -diagram may be described as flat or, near the upper boundary of the region, wavy.

5. Turbulence with surface tension dominant and gravity unimportant

Region 1 of figure 4 has large Froude number and small Weber number, giving relatively small-scale turbulence: length scales of the order 1 cm and less for water. Here surface tension is able to maintain the cohesion of the liquid but gravity fails to keep the surface flat. The result is smooth rounded surfaces. If the turbulence is below the critical region then there is not much wave generation and we describe the surface as knobbly. This type of flow is illustrated in figure 5 with three views of a hydraulic jump at the base of a weir in a laboratory flume. The knobbly nature of the surface is evident. The typical length scale is around 1 cm. Other concurrent experiments, partly described in Peregrine & Svendsen (1978) showed that the turbulence was intense, having a length scale that was very small compared with the overall size of the breaker. See figure 2. The scale of the turbulence that is most effective at disturbing the surface can best be seen in figure 5(a) which is an oblique view from above. Recent studies of turbulence by particle image velocimetry (PIV) visualization (e.g. Lin & Rockwell 1995; Sheridan, Lin & Rockwell 1997; Pogozelski, Katz & Huang 1997; Dabiri & Gharib 1997; Dong, Katz & Huang 1997) show instantaneous views of similar but weaker flows, which also show the transition to turbulence. However, these authors give little information on the surface shape and its irregular motion.

Note that this is also the regime of micro-breakers, which are small breaking waves similar in scale to the hydraulic jump of figure 5, and smaller. These are ubiquitous on a water surface whenever winds stronger than the lightest are blowing. The micro-breakers are likely to be the major avenue for heat and mass transfer between ocean and atmosphere. Although these micro-breakers are evident to the naked eye, it is only in recent years that their existence and importance has been noticed (e.g. Banner & Peregrine 1993; Melville 1996; Banner & Peirson 1998).

The strength of turbulence beneath even very small breakers can be quite striking as is shown in figure 6 where a bore of height a very few millimetres is travelling into still water of a similar depth which is laden with small aluminium flakes to aid visualization.

We have already made an estimate of the upper boundary of this region where the surface commences to break up as the turbulence becomes stronger. However, even before breakup there can be strong interaction between the free surface and the underlying flow: we see from Lin & Rockwell (1995) and Longuet-Higgins (1992) that the shedding of vorticity from the trough of a capillary wave can be important and can generate turbulence. Further, the form of the limiting Crapper wave indicates that the critical Weber number we deduce from it may be particularly appropriate for the entrainment of bubbles from the free surface. If the surface pinches off a small cylindrical bubble of air, the capillary forces will rapidly break it up into small spherical bubbles.

The value of We_c evaluated from the limiting Crapper wave is more than three

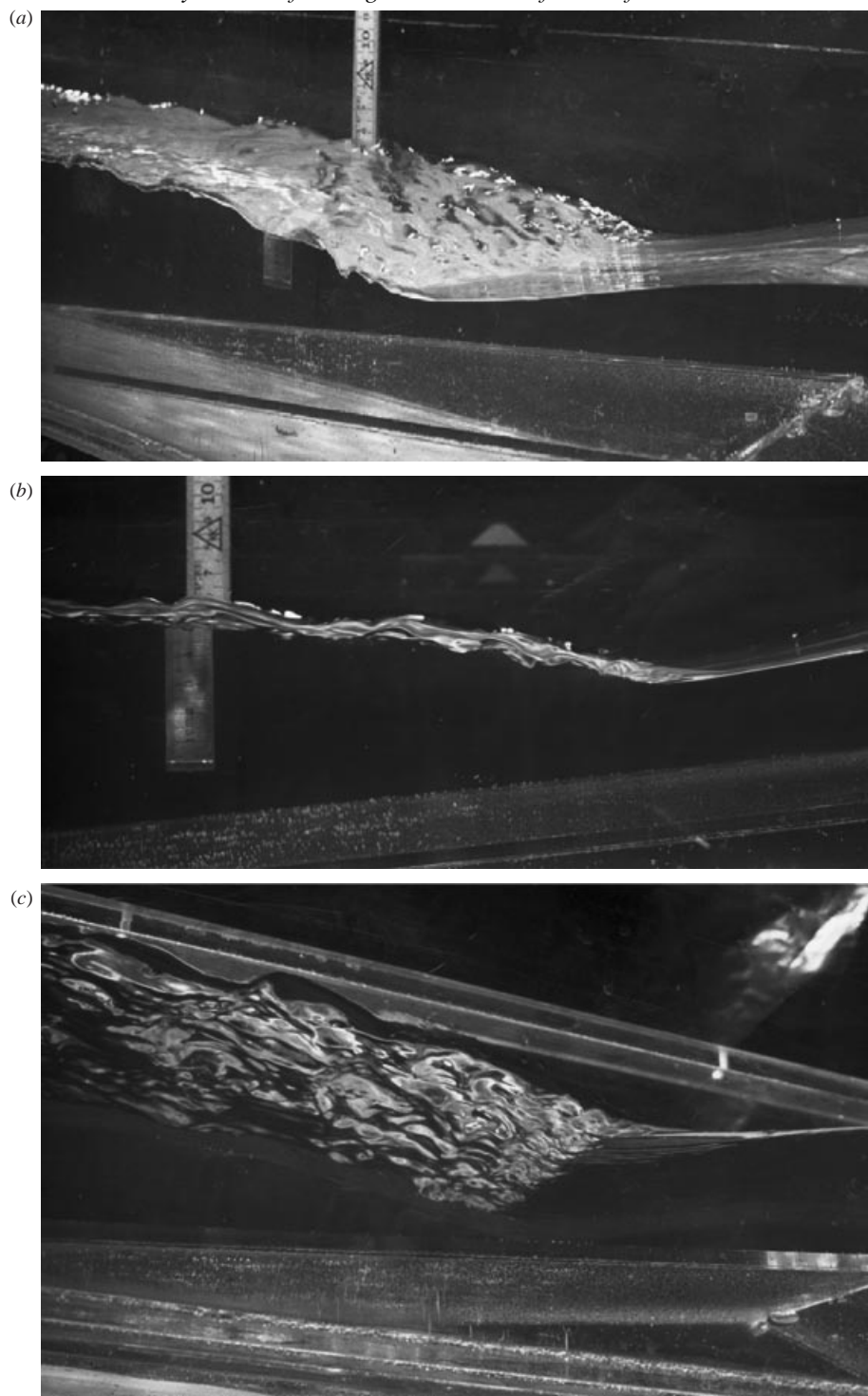


FIGURE 5. Knobby flow. Oblique view from above (*a*), side view (*b*) and view from below (*c*) of a hydraulic jump fed by flow over a weir. The incoming flow has a depth of about 4 cm. The vertical ruler, visible in the upper two photographs, is marked in centimetres. These photographs are from experiments at the Technical University of Denmark upon which the discussions of Peregrine & Svendsen (1978) were based.

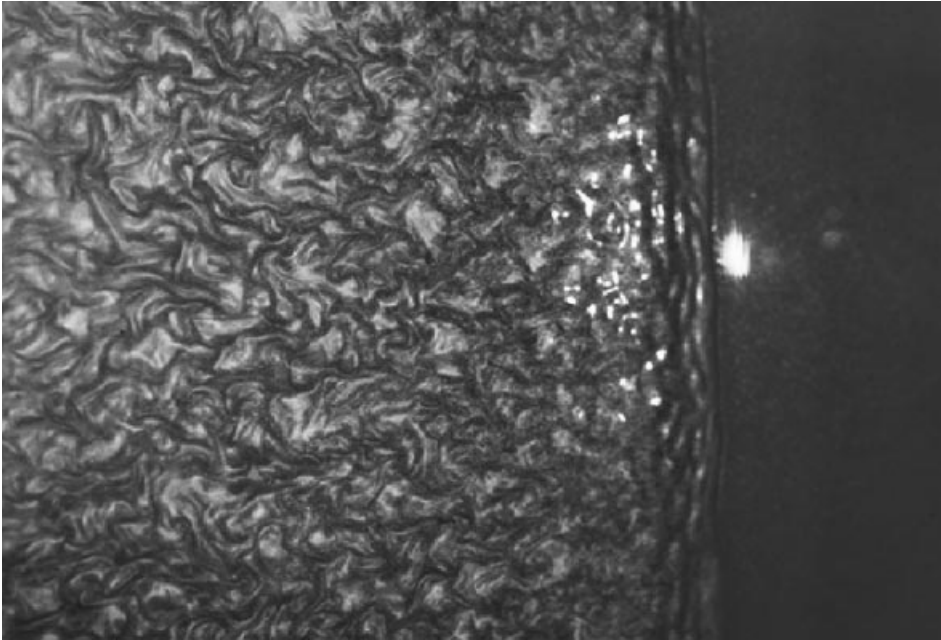


FIGURE 6. Small bore of a few millimetres height in water of comparable depth with flow visualization using aluminium flakes. The field of view is approximately 30 cm long.

times larger than that obtained for splashing in §3 in which we approached the problem from another direction by estimating the energy needed to form a drop or a scar. This shows that we can only estimate both We_c and Fr_c with a large margin of uncertainty. To this uncertainty, due to the modelling, we have to add that turbulence is essentially three-dimensional and we know little about the limiting configurations of three-dimensional capillary waves, despite a recent surge of papers on nonlinear aspects of Faraday waves, e.g. Miles (1993); Decent & Craik (1995); Jiang *et al.* (1996); Kim & West (1997), Goodridge *et al.* (1997). A range of experimental studies are needed to test the value of our parametric description by quantifying the various regimes that can be seen.

6. Very strong turbulence

When turbulence is so strong that neither surface tension nor gravity can maintain surface cohesion the flow breaks up into drops and bubbles, region 2 of the (L, q) -plane. This is an essentially two-phase flow region. However, there are many aspects of such flows that are not within the usual topics studied in two-phase flow, which tends to be much influenced by the need to study flow in pipes. Although the drops and bubbles are dominated by surface tension the capillary energy associated with them is still much less than the overall turbulent energy from which they are formed. At a free surface there is the growth and decay of the strong turbulence to consider as well as the structure of the transition between gas and liquid.

When strong turbulence, generated elsewhere, meets a free surface the fluctuating eddies are no longer restrained by the inertia of surrounding non-turbulent liquid. Thus the surface ‘erupts’ as any blob of liquid approaching the surface maintains its speed. Such an eruption may be exemplified by the ‘rooster tail’ seen at the rear



FIGURE 7. A 'rooster tail' generated by a Seacat. The lower right of the photograph is where the highly turbulent propulsive jet has just come out from beneath a hull.

of high-speed vessels as the turbulent flow from their driving mechanism meets the free surface. Sometimes the flow is sufficiently well organized that some of the 'tail' is due to a discrete splash, but in general one can expect substantial spray to heights of $q^2/2g$ (see figure 7). This contrasts with the weak turbulence case of an almost flat surface. For weak turbulence the vertical velocity fluctuations w approach zero at the free surface; on the other hand for strong turbulence w can be expected to be larger than u and v since the horizontal fluctuations are more constrained by the inertia of the surrounding liquid. This complete disparity in the variation of w gives the clearest indication that different surface regimes need different approaches in developing turbulent models.

Consideration of the structure of these violent flows leads to examination of the breakup of blobs of water. This of course partly depends on how the turbulence is generated; however, as Peregrine (1981) pointed out, a blob of water thrown away from the bulk deforms under the influence of the inertia of the residual motion within the water mass, thus any portion of the surface which commenced with an outward motion is no longer restrained and continues its outward motion. Thus, the water soon spreads into sheets and filaments which rapidly breakup once their shortest length scale brings them into the range of capillary forces.

The capillary instability of a liquid jet has been studied since the 19th century and most of the experimental and analytical work was summarized by Rayleigh (1945). A good review on drop formation by disintegration of jets (or sheets) is given by Clift *et al.* (1978, § 12). Though quantitative analysis of critical parameters for drops splitting in air is rather common in the literature this is not the case for drop generation by

primary breakup of a free surface by turbulence. Only a few works (e.g. Dai, Hsiang & Faeth 1996) report measurements of drops sizes and relate them to turbulence.

For flows which are only just splashing the trajectory of individual drops is often sufficiently short that it is described well by an inviscid trajectory under gravity. However, if there is significant gas motion or the violence of the turbulence leads to smaller drops, or the trajectories are longer because of a large overall scale, drag from the air becomes important. This is clearly seen in experiments by Rao, Seetharamiah & Gangadharaiah (1970) and Gangadharaiah, Rao & Seetharamiah (1970) on self-aerated flow down spillways. In that case the air drag slows the water drops, and the drops induce an air flow. Such induced flows of air are usually very evident near large waterfalls.

The spread of gas downward and the formation of bubbles is usually less obvious to the external observer, though bubbles are in some ways more important than drops since they have longer lifetimes. The distribution of bubble sizes not only depends on the strength of the turbulence but on liquid properties that have yet to be fully determined, see Weissenborn & Pugh (1996). Scott (1976) demonstrates clearly how just 1% of salt in water makes a substantial difference to bubble size.

Less well known than the evolution of bubble size is the transition between 100% gas and 100% liquid. On consideration it is self-evident that there is some bounding surface, when moving from the liquid side, where the liquid ceases to be connected. Similarly when moving from the gas side there is a surface bounding the connected gas. There is a strong likelihood that these are different boundaries and that there is a region where both gas and liquid are both fully connected but interpenetrating. This is an example of the 'percolation problem', which has a long history (see Grimmett 1989).

Further, the spread of drops and bubbles from the mean interface can differ considerably. The drops are projected to a distance that depends to a large extent on their initial velocity as they are formed in the two-phase layer. Thereafter, unless there are some strong flows in the gas, they travel no higher than this initial energy permits against gravity and drag effects. On the other hand bubbles once formed have little persistent inertia and a small rise velocity so that they are likely to be drawn down to at least a depth L , and the smaller bubbles are drawn to much greater depths, e.g. Thorpe (1992) and Thorpe, Bowyer & Woolf (1992) give reviews of the distribution of bubbles in the sea.

However, for considering dynamical effects on turbulence, the main emphasis of our work, the extremes of the bubble or drop distribution are of little relevance. Other parameters become important, in particular the rise velocity of the typical bubbles, or clumps of bubbles, compared with the evolution time scales and length scales of the turbulence. Bubbles that evolve from enveloped air masses, after an initial strong turbulent mixing have a diameter of approximately 5 mm in fresh water and 1 mm in salt water, Scott (1976). The overall scale of a breaker or turbulent flow is also important, for example air escapes from a 10 cm breaker as it passes, and has little time to influence the turbulence, whereas clouds of entrained air bubbles can be giving buoyancy to the turbulent eddies behind a 5 m breaker long after the breaker has passed by.

7. Gravity-dominated turbulence

Region 3 of our (L, q) -diagram has gravity dominating the turbulence, $Fr \ll 1$, with weak surface tension, $We \gg 1$. It is by far the commonest state since it applies

to almost all terrestrial water bodies with flow: streams, rivers, seas and oceans. The free surface is essentially flat or nearly so. Linearized boundary conditions are generally satisfactory. However, there is a range of interesting flow properties in this regime as the turbulent energy is increased towards the splashing case. These are local effects and their significance in various applications is not well determined. These phenomena arise since the turbulence has more than adequate energy to disturb the free surface, but only at length scales which are smaller than the main turbulent eddies. At the edge of the eddies, where strong shear develops, or the eddy boundary is moving or there is a strong surface convergence, a shorter length scale, $L/10$ or $L/100$ or even less, becomes important. If k , or $\frac{1}{2}q^2$, retains more or less the same value at this shorter scale then it is readily seen that the corresponding horizontal line from a point in region 3 of the (L, q) -plane leading to smaller values of L can often reach the boundary with the splashing region.

The most characteristic features of these smaller regions are waves, vortex dimples and scars. In every case these can give rise to localized surface breaking, and hence introduce to the turbulent flow aspects which are not present in the single-phase case. Both gas entrainment and vorticity generation are greatly enhanced by any surface breaking. Hence these small-scale regions may be important features of the flow even when they form a very small fraction of an otherwise flat, smooth and coherent surface.

The surface flow due to the turbulence may also have a strong effect on short waves propagating on the surface, often causing breaking.

In addition, there are also circumstances when the surface is particularly 'sensitive' to disturbances beneath the surface. This might be the explanation of some remarks by Chanson (1996), when discussing self-aerated flows in channels of moderate to gentle slope, which seem to be strange. Generally self-aeration occurs when the turbulent boundary layer growing from the bed of the channel meets the surface. However, on gentle slopes the aeration commences well before the boundary layer reaches the surface. The photograph illustrating this puzzling behaviour (Chanson 1996, figure 11-2) shows significant smooth surface motions before aeration occurs. A likely cause of these motions is the underlying turbulence. The entraining 'billows' at the surface of the turbulent boundary layer are moving down the channel at a speed intermediate between the speed of surface water and the stationary bed. The almost irrotational flow of the stream over these billows may have a Froude number relative to the billows that is close to unity. For such near-critical free-surface flows small disturbances can generate a disproportionately large response at the free surface. Apparently this leads to breaking appreciably before there is any direct contact between the rotational turbulent flow and the surface.

Where the significant smaller scales are near those of capillary waves the surface can have many groups of ripples. These often have the nature of capillary bores and might be useful for interpreting the subsurface flow. Longuet-Higgins (1996) discusses one particular case, and we note their occurrence in connection with scars below.

All these deformations of the free surface are useful in giving some indication of the nature of the turbulent flow beneath the surface. However, when the surface features are ripples or waves care must be taken in interpreting their implications. Waves are strongly affected by currents and can become prominent because of focusing, either in space or in space-time. This means that there may be a significant displacement between the surface current feature that affects waves or ripples and the position of steepest waves. Strong vortex dimples arise from concentrations of vertically oriented vorticity. However, they are unlikely to be important for most turbulent flows because



FIGURE 8. Scarified flow in a ship's wake. On the overall scale of the wake the surface shows little disturbance, but at the edges of major upwellings there is strong disturbance at a much smaller scale.

they are effectively point-like objects whereas breaking waves and scars are more line-like on the surface. Although scars seem to be very important they have received little direct study. We thus digress in the next section to give a partial description of this flow feature and related flows.

8. Scars, turbulent and laminar

Scars have already been referred to in earlier sections. At their most developed stage scars occur where flow on at least one side is downward causing a trough in the surface, e.g. at the edge of upwelling boils, or adjacent to submerged horizontal vortices. They are often evident in ship's wakes where strong trailing vortices shed from the hull, or caused by propeller motion, sometimes cause long scars in a ship's wake. See figure 8 where scars can be seen at two different scales. There is both a main wake structure, upwelling smoothly at the centre giving two large-scale scars at the one-third positions across the wake, and scars at the boundaries of the larger eddies. Their common feature is that they correspond to a flow with a downward separation from the free surface.

Consider two-dimensional flows, for simplicity. An ordinary laminar flow separation off a smooth surface with a free-slip condition leads to a streamline that leaves the surface from a stagnation point, and descends at an angle to the surface, e.g. perpendicular to the surface for irrotational flow. However, there are two other distinct types of separation that may be found in laminar flow at a free surface. For symmetrical flow, Jeong & Moffatt (1992) solved for the downward separating flow and found that as the relative effect of surface tension decreases the stagnation point is drawn downwards beneath the mean surface level and the curvature at the bottom

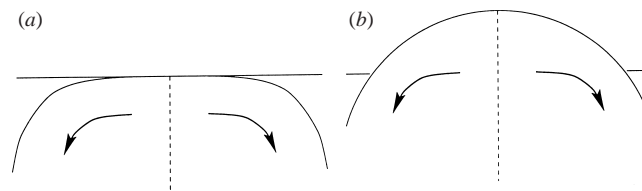


FIGURE 9. Examples of inviscid flows with vortex sheets leaving the free surface. In this idealized limit the flow at the outer edges of the free surface in each diagram is at rest.

of the resulting trough rapidly increases. The result is that for reasonable strength flows the curvature becomes comparable with the ordinarily neglected length scale of surface transition from typical liquid to typical gas. In effect a cusp can form since finer details can only be resolved by a better model of the surface layer that is being drawn down, see Shikhmurzaev (1998) for example. Such a cusp line is a laminar version of a scar, and it seems likely that a moderate amount of asymmetry in the flow can give similar results. Note that the stagnation point flow, in the normal continuum mechanics model, does not permit fluid particles to leave the surface. A cusp type of flow does, hence a cusp line is an exceptionally effective place for gas liquid transfers, and if a cusp is asymmetric it may be equally effective at entraining vorticity into the liquid, a point that has not been noticed by several recent authors discussing vortex generation at a free surface (Yeh 1994; Rood 1995). Cusp-like lines may also be seen in figure 3.

There is a further type of separation that occurs on free surfaces and is entirely asymmetrical: at its weakest it is known as a Reynolds ridge (Reynolds 1881; see also McCutchen 1970; McDowell & McCutchen 1971 and Scott 1982). Here the surface flow is slowed down, perhaps by gradients of surface-active agents, but only a very thin layer of fluid is at rest. Boundary layer analysis of a weak flow of this sort is presented in Harper & Dixon (1974). However, to date these analyses have required an incoming velocity below the minimum phase speed for capillary-gravity surface waves. At greater speeds ripples form, and for greater speeds of flow the ripples become shorter and steeper and break. The flow then has the nature of a scar. There have been few or no experiments to quantify this sequence of events, but it may be seen on small streams flowing over an irregular bed.

These flows can also be viewed from another limit: inviscid flows with vortex sheets. A couple of examples are sketched in figure 9. Figure 9(a) corresponds to the extension of the Reynolds ridge flows. A vortex sheet leaves the free surface tangentially and separates a stagnant region from a descending flow: thus it is a typical free streamline. Peregrine (unpublished, 1973) used Hopkinson's (1898) conformal-mapping approach to find the solution for a flow like this from a line source while investigating extensions of his study of a line source beneath a free surface (Peregrine 1972). Gravity is supposed to be strong enough to restrain any surface deflections. On the other hand figure 9(b) shows a stronger upwelling flow 'falling through' the surface. At its extreme this latter example is exemplified by a small waterfall or low fountain.

9. Discussion

We have given a descriptive account of some of the features that arise when strong, or not so strong, turbulence is present at a free surface. Figure 10 shows an (L, q) -

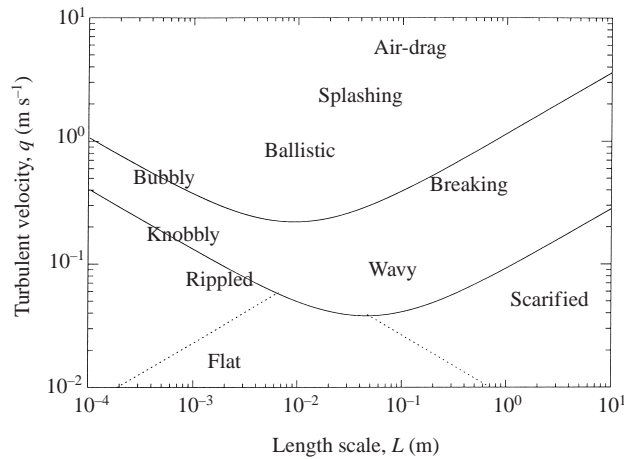


FIGURE 10. Diagram of the (L, q) -plane with tentative descriptions of the flow regimes. The transition region from the upper and lower bounds obtained from equations (3.1) and (3.2) is indicated.

diagram with adjectives placed in appropriate regions to summarize the flow types we have discussed. It is clear from our above account that the identification of the appropriate regions is rather tentative. This is due to the absence of experimental measurements of appropriate quantities. Indeed, we hope that our attempt here to identify such regions will stimulate work to further characterize these flow types and their features. There is no doubt that we have left out some important features. Air is one of them: in figure 10 we do indicate a region where large-scale splashing leads to the effect of air drag being significant on the resulting drops. On the other hand air may be more important for the fluid dynamics when mixed in with the liquid. In most of this paper and the following papers we ignore it in the interests of simplification.

As well as considering each type of flow, it is useful to set particular flows into this general context. Few real flows correspond to just one spot in the (L, q) -diagram. Flow down a steep slope might in certain circumstances reach an equilibrium corresponding to one point in the diagram, but this would usually imply a high Froude number giving the potential to develop roll waves. Mechanically stirred flows in a vessel closely fitting the stirring mechanism may be the best way to obtain flow with one value for (L, q) . For most flows the varying character of the turbulence can be characterized by surface trajectories obtained by following the flow across the (L, q) -diagram. In flows where water initially on the free surface meets turbulence its trajectory sweeps across the (L, q) -diagram and back again along the paths marked ABC and PQRS in figures 12 and 15, discussed below.

Consider a hydraulic jump or quasi-steady spilling breaker, as shown in figure 11. One possible trajectory is that marked ABCD in both the photograph of figure 11 and the parameter space in figure 12. Water approaching a jump would generally have weak turbulence of a length scale corresponding to the depth of water, A. As it meets the foot of the breaker it suddenly is in very strong splashing turbulence, B: the dashed line in figure 12 is from the large value of L to a much smaller value with high turbulent velocities. Individual water particles then spread extremely quickly to the whole turbulent layer, but we shall follow our notional surface blob. On the front face of the wave or jump, there is a reduction in turbulent energy as the surface is followed, against a small mean downward velocity, to the crest of the wave. At the same time, the scale of the turbulent eddies increases, so that the trajectory meets the



FIGURE 11. A bore on the beach at Scripps Institute of Oceanography. The letters ABCD are related to the points so labelled in the parameter space of figure 12.

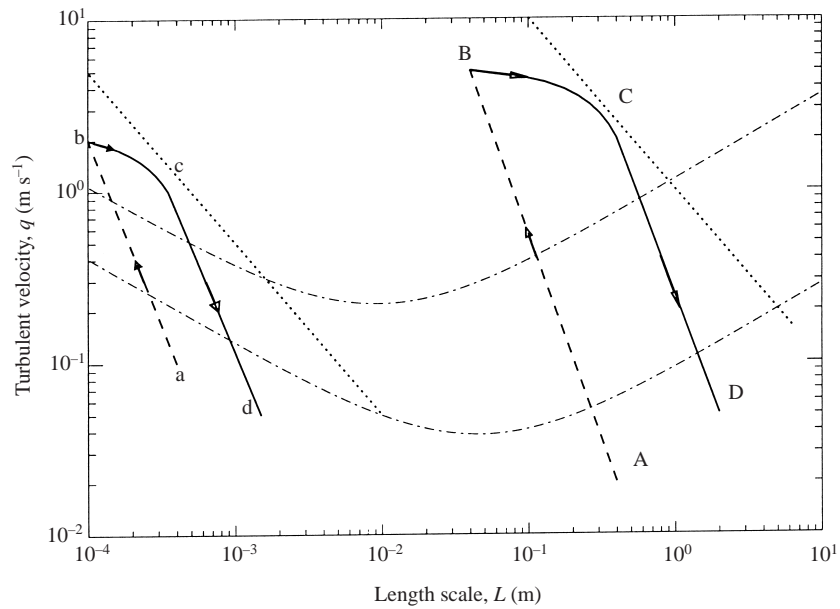


FIGURE 12. Diagram of the (L, q) -plane with trajectories representative of the flow in a hydraulic jump or spilling breaker. The dotted line corresponds to an upper limit to the turbulent energy for each of the two jumps trajectories, ABCD and abcd shown.

boundary of the stable region, and eventually the turbulence becomes weak with a length scale comparable with the new greater depth, D. In sketching the shape of a trajectory like ABCD several considerations come to mind.

The line AB represents a jump in the state of the water, hence the use of a dashed

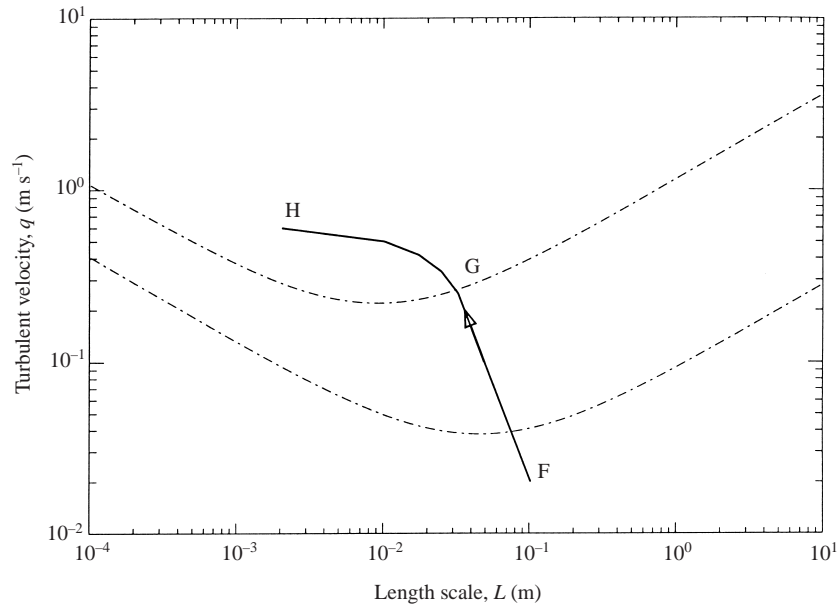


FIGURE 13. Diagram of the (L, q) -plane with a trajectory representative of the flow in a spillway. The points F, G and H represent the initial flow and points further down the spillway respectively.

line: but what determines the location of B in the (L, q) -diagram? The value of q must be roughly equal to the speed of advance of the breaker relative to the water immediately in front of it. The length scale L at most corresponds to the size of the blobs falling forward to the foot of the breaker. As discussed in Part 2, § 8, the irregularities at the foot of a breaker, formed by these falling blobs, are important features in the modelling of the foot of a breaker. We call them 'toes'. An average over these toes to obtain a mean position also gives a mean height. At present no one seems to have measured such blobs, toes or mean height. Observation (D.H.P.) indicates that they are not always a simple fraction of the breaker height.

The trajectory BC is less certain. Is the turbulence most intense at its inception? If not should the trajectory rise a little? Probably not: although the total production of turbulence may be greater a short distance from the foot at B, it is then being spread over a greater volume of water. Then even before the crest, unless the breaker is unsteady and gaining in strength, the turbulence begins to decay as it spreads further and increases its length scale. The shape of this part of the trajectory can be bounded by consideration of a limiting case. If there is no dissipation then we need to conserve turbulent energy per unit width of the flow and hence $L^2 q^2$ must be constant. Thus our trajectory must 'fall through' the hyperbolas of q proportional to $1/L$. This can be quantified further for the hydraulic jump where we know the total energy dissipation and hence the hyperbola corresponding to the maximum energy density, which gives an absolute upper bound, sketched in figure 12 as a dotted line. For hydraulic jumps on a small scale, such as shown in figure 5, the trajectory shown as abcd is likely.

A somewhat different trajectory is followed in the (L, q) -diagram for flows where the turbulence comes from below the free surface, such as for a submerged jet or flow down a spillway. We first discuss the latter since this often occurs with little lateral variation. Flow over the crest of a spillway usually has a low level of turbulence, denoted by F in figure 13. As the flow accelerates down the spillway the boundary



FIGURE 14. The surface traces of a submerged jet entering the River Avon at Bristol. This view covers about 10 m from the river bank which is at the lower edge of the photograph.

layer increases in thickness, turbulent eddies meet the surface and soon lead to splashing, G. The length scale L is shown as decreasing since the flow is accelerating and hence the depth of water decreases until the surface breaks up. Thereafter, the dispersed water gives a greater depth, but it seems unlikely that the length scale of turbulence can increase in a corresponding manner if the surface breaks up violently. Once splashing occurs length scales of the water can reduce drastically, to H, as the water breaks up into drops. On the other hand, if the surface is not so violently disturbed, the very long, and slowly increasing, length scale of roll waves can appear.

A horizontally oriented subsurface jet, such as has been studied by Walker *et al.* (1995) and Hong & Walker (2000), and as is shown in figure 14, gives a different trajectory in the (L, q) -diagram. This is sketched in figure 15 for a trajectory along the water surface above the centreline of the jet. Initially the surface is little disturbed, P, and as the turbulent eddies reach the surface it may become more or less strongly disturbed, Q to R. Eventually the turbulence decays, to S. All the time the length scale of the turbulence is increasing since there is no further input of turbulent energy.

The subsurface jet flow and some spillway flows illustrate an ambiguity in the (L, q) -diagram we are using. It concerns the region just below the stability boundary where we describe both wavy and scarified regimes. In following a trajectory from F to G and from P to Q as turbulence comes to the surface, the surface is first disturbed by the irrotational velocity fluctuations outside the turbulent region. This gives a wavy surface which generally has very small displacements. On the other hand as a flow trajectory crosses the stability boundary in the other direction, e.g. R to S, and also B to C in figure 12 the flow usually has few waves but is scarified.

For the case of a turbulent water jet emerging from a pipe into air the only stabilizing effect is surface tension. Thus we expect that except for the smaller jets with relatively gentle turbulence the flow just proceeds to disintegrate. We note that

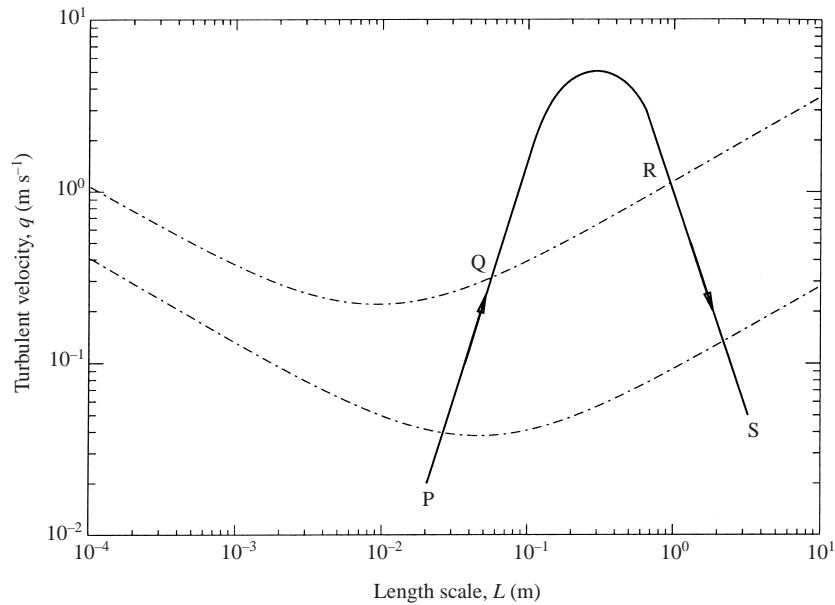


FIGURE 15. Diagram of the (L, q) -plane with a trajectory representative of the surface disturbance due to the flow of a submerged jet. PQRS are points along the surface trace of the centreline of the jet.

Lasheras & Hopfinger (2000) review liquid jet instability and for jets with annular gas flows make use of a (We, Re) parameter space.

10. Conclusion

In this paper we have described some of the features that arise when there is strong turbulence at a free surface. A wide range of behaviour can occur and by considering the stabilizing influences of gravity and surface tension we give a structure in which to consider these flows based on the length scale and energy of the turbulence. As mentioned above this is not an unambiguous way of describing the flows; however, as a first step it has the merit that it reveals where further study is needed. We hope that this paper may act to stimulate studies, such as experiments and idealized numerical and analytical models, relating turbulence to the surface disturbances it causes.

The work presented here is a preliminary to the following papers which are concerned with modelling such flows. In Part 2 we derive averaged boundary conditions for turbulent flows. As usual, for turbulence, there are averaged terms for which a closure hypothesis is required. One aim of this introductory paper is to indicate that the variety of free-surface flows is such that it is likely that effective closures should differ for differing regimes, and such closures might be parameterized in the (q, L) -space, if q and L are suitably chosen.

Support from the European Commission, Directorate General XII, contracts ER-BCHBICT930678, MAS2-CT92-0047 and MAS3-CT97-0081; the U.K. Engineering and Physical Sciences Research Council, Grant No. GR/H/96836, the Italian MURST Grant "Processi Vorticosi, Turbolenti e Caotici", and the USA Office of Naval Research NICOP Grant No. N00014-97-1-0791 is gratefully acknowledged. Referees are thanked for their helpful comments.

REFERENCES

- BANNER, M. L. & PEIRSON, W. L. 1998 Tangential stress beneath wind-driven air–water interfaces. *J. Fluid Mech.* **364**, 115–145.
- BANNER, M. L. & PEREGRINE, D. H. 1993 Wave breaking in deep water. *Ann. Rev. Fluid Mech.* **25**, 373–397.
- BANNER, M. L. & TIAN X. 1998 On the determination of the onset of breaking for modulated gravity waves. *J. Fluid Mech.* **367**, 107–137.
- BLANCO, A. & MAGNAUDET, J. 1995 The structure of the axisymmetric high-Reynolds number flow around an ellipsoidal bubble of fixed shape. *Phys. Fluids* **7**, 1265–1274.
- BOETTCHER, E. J., FINEBERG, J. & LATHROP, D. P. 2000 Turbulence and wave breaking effects on air–water gas exchange. *Phys. Rev. Lett.* **85**, 2030–2033.
- BORUE, V., ORSZAG, S. A. & STAROSELSKY, I. 1995 Interaction of surface waves with turbulence: direct numerical simulations of turbulent open-channel flow. *J. Fluid Mech.* **286**, 1–23.
- BOYEV, A. G. 1971 The damping of surface waves by intense turbulence. *Izv. Atmos. Ocean. Phys.* **7**, 31–36.
- BREMEN, R. & HAGER, W. H. 1989 Experiments in side-channels spillways. *J. Hydr. Engng ASCE* **115**, 617–635.
- BROCCHINI, M. 1996 Flows with freely moving boundaries: the swash zone and turbulence at a free surface. PhD Dissertation. University of Bristol.
- BROCCHINI, M. & PEREGRINE, D. H. 2001 The dynamics of strong turbulence at free surfaces. Part 2. Free-surface boundary conditions. *J. Fluid Mech.* **449**, 255–290.
- BROCCHINI, M. & PEREGRINE, D. H. 2002 The dynamics of string turbulence at free surfaces. Part 3. A model for a spilling breaking wave. (in preparation).
- CHANSON, H. 1993 Self aerated flows on chutes and spillways. *J. Hydr. Res.* **119**, 220–243.
- CHANSON, H. 1995 Predicting oxygen-content downstream of weirs, spillways and waterways. *Proc. Inst. Civil Engrs – Water, Maritime & Energy* **112**, 20–30.
- CHANSON, H. 1996 *Air Bubble Entrainment in Free-Surface Turbulent Shear Flows*. Academic.
- CHEN, Y., GLIMM, J., SHARP, D. H. & ZHANG, Q. 1996 A two-phase flow model of Rayleigh–Taylor instability. *Phys. Fluids* **8**, 816–825.
- CLIFT, R., GRACE, J. T. & WEBER, M. E. 1978 *Bubbles, Drops and Particles*. Academic.
- COKELET, E. D. 1977 Steep gravity waves in water of arbitrary uniform depth. *Phil. Trans. R. Soc. Lond. A* **286**, 183–230.
- COLEMAN, J. M. 1969 Brahmaputra River: channel processes and sedimentation. *Sediment. Geol.* **3**, 129–239.
- CRAPPER, G. D. 1957 An exact solution for progressive capillary waves of arbitrary amplitude. *J. Fluid Mech.* **2**, 532–540.
- DABIRI, D. & GHARIB, M. 1997 Experimental investigation of the vorticity generation within a spilling breaking wave. *J. Fluid Mech.* **330**, 113–139.
- DAI, Z., HSIANG, L.-P. & FAETH, G. 1996 Spray formation at the free surface of turbulent bow sheets. *Proc. 21st Symp. on Naval Hydrodynamics*, vol. 1, pp. 197–211.
- DAVIES, J. T. 1972 *Turbulence Phenomena*. Academic.
- DAVIES, J. T. & DRISCOLL, J. P. 1974 Eddies at free surfaces, simulated by pulses of water. *Indust. Engng Chem. Fundam.* **13**, 105–109.
- DECENT, S. P. & CRAIK, A. D. D. 1995 Hysteresis in Faraday resonance. *J. Fluid Mech.* **293**, 237–268.
- DOLD, J. W. & PEREGRINE, D. H. 1986 An efficient boundary-integral method for steep unsteady water waves. *Numerical Methods for Fluid Dynamics II* (ed. K. W. Morton & M. J. Baines), pp. 671–679. Oxford University Press.
- DONG, R. R., KATZ, J. & HUANG, T. T. 1997 On the structure of bow waves on a ship model. *J. Fluid Mech.* **346**, 77–115.
- DOUGLAS, S. L. & WEGGEL, J. R. 1988 A laboratory experiment on the influence of wind on nearshore breaking waves. *Proc. 21st Intl Conf. Coastal Engng ASCE*, vol. 1, 632–643.
- DUNCAN, J. H. & DIMAS, A. A. 1996 Surface ripples due to steady breaking waves. *J. Fluid Mech.* **329**, 309–339.
- DUNCAN, J. H., QIAO, H. B., PHILOMIN, V. & WENZ, A. 1999 Gentle spilling breakers: crest profile evolution. *J. Fluid Mech.* **379**, 191–222.

- GANGADHARAI AH, T., RAO, N. S. L. & SEETHARAMIAH, K. 1970 Inception and entrainment in self-aerated flows. *J. Hydr. Engng. ASCE* **96**, 1549–1565.
- GIBSON, M. M. & RODI, W. 1989 Simulation of free surface effects on turbulence with a Reynolds stress model. *J. Hydr. Res.* **27**, 233–244.
- GOODRIDGE, C. L., SHI, W. T., HENTSCHEL, H. G. E. & LATHROP, D. P. 1997 Viscous effects in droplet-ejecting capillary waves. *Phys. Rev. E* **56**, 472–475.
- GRIMMETT, G. R. 1989 *Percolation*. Springer.
- HANDLER, R. A., SWEAN, T. F., LEIGHTON, R. I. & SWEARINGEN, J. D. 1993 Length scales and the energy balance for turbulence near a free surface. *AIAA J.* **31**, 1998–2007.
- HARPER, J. F. & DIXON, J. N. 1974 The leading edge of a surface film on contaminated water. *Proc. 5th Australasian Conf. on Hydraulics & Fluid Mech.* vol. 2, pp. 499–505.
- HASSELMANN, K. 1971 On the mass and momentum transfer between short gravity waves and larger-scale motions. *J. Fluid Mech.* **50**, 189–205.
- HODGES, B. R. & STREET, R. L. 1999 On the simulation of turbulent nonlinear free-surface flows. *J. Comput. Phys.* **151**, 425–457.
- HOGAN, S. J. 1979 Some effects of surface tension on steep water waves. *J. Fluid Mech.* **91**, 167–180.
- HONG, W.-L. & WALKER, D. T. 2000 Reynolds-averaged equations for free-surface flows with application to high-Froude-number jet spreading. *J. Fluid Mech.* **417**, 183–209.
- HOPKINSON, B. 1898 On discontinuous fluid motions involving surfaces and vortices. *Proc. Lond. Math. Soc.* **29**, 142–164.
- HUNT, J. C. R. & GRAHAM, J. M. R. 1978 Free stream turbulence near plane boundaries. *J. Fluid Mech.* **84**, 209–235.
- JEONG, T. T. & MOFFATT, H. K. 1992 Free-surface cusps associated with flow at low Reynolds-number. *J. Fluid Mech.* **241**, 1–22.
- JIANG, L., TING, C. L., PERLIN, M. & SCHULTZ, W. W. 1996 Moderate and steep Faraday waves: instabilities, modulation and temporal asymmetries. *J. Fluid Mech.* **329**, 275–307.
- KIM, W. & WEST, B. J. 1997 Chaotic properties of internal wave triad interaction. *Phys. Fluids* **9**, 632–647.
- KOMORI, S., MURAKAMI, Y. & UEDA, H. 1989 The relationship between surface-renewal and bursting motions in an open channel flow. *J. Fluid Mech.* **203**, 103–123.
- LAMB, H. 1932 *Hydrodynamics*. Cambridge University Press.
- LASHERAS, J. C. & HOPFINGER, E. J. 2000 Liquid jet instability and atomisation in a coaxial gas stream. *Ann. Rev. Fluid Mech.* **32**, 275–308.
- LEIGHTON, R. I., SWEAN, T. F., HANDLER, R. A. & SWEARINGEN, J. D. 1991 Interaction of vorticity with a free surface in turbulent open channel flow. *AIAA Paper* 91-0236.
- LIN, J. C. & ROCKWELL, D. 1995 Evolution of a quasi-steady breaking wave. *J. Fluid Mech.* **302**, 29–44.
- LONGUET-HIGGINS, M. S. 1992 Capillary rollers and bores. *J. Fluid Mech.* **240**, 658–679.
- LONGUET-HIGGINS, M. S. 1996 Surface manifestations of turbulent flow. *J. Fluid Mech.* **308**, 15–29.
- LUGT, H. J. & OHRING, S. 1992 The oblique ascent of a viscous vortex pair toward a free-surface. *J. Fluid Mech.* **236**, 461–476.
- MADSEN, P. A. & SVENDSEN, I. A. 1983 Turbulent bores and hydraulic jumps. *J. Fluid Mech.* **129**, 1–25.
- MARON, D. M., YACOUB, N., BRAUNER, N. & NAOT, D. 1991 Hydrodynamic mechanisms in the horizontal slug pattern. *Intl J. Multiphase Flow* **17**, 227–245.
- MCCUTCHEM, C. W. 1970 Surface films compacted by moving water: demarcation lines reveal film edges. *Science* **170**, 61–64.
- MCDOWELL, R. S. & MCCUTCHEM, C. W. 1971 The Thoreau–Reynolds ridge, a lost and found phenomenon. *Science* **172**, 973.
- MEIER, G. E. A., KLOPPER, A. & GRABITZ, G. 1992 The influence of kinematic waves on jet break down. *Exps. Fluids* **12**, 173–180.
- MELVILLE, W. K. 1996 The role of surface-wave breaking in air-sea interaction. *Ann. Rev. Fluid Mech.* **28**, 279–323.
- MERCER, G. N. & ROBERTS, J. 1992 Standing waves in deep water: their stability, and extreme form. *Phys. Fluids A* **4**, 259–269.

- MICHEL, V. & LOVELEY, M. 1953 Some prototype observations of air entrained flow. *Proc. 5th IAHR Congress, Minnesota*, pp. 403–414.
- MILES, J. 1993 On Faraday waves. *J. Fluid Mech.* **248**, 671–683.
- NEZU, I. & NAGAKAWA, H. 1993 *Turbulence in Open Channel Flows*. Intl. Assoc. Hydraulic Res. Monograph. Balkema.
- ÖLMEZ, H. S. & MILGRAM, J. H. 1992 An experimental-study of attenuation of short water-waves by turbulence. *J. Fluid Mech.* **239**, 133–156.
- PAN, Y. & BANERJEE, S. 1995 A numerical study of free-surface turbulence in channel flow. *Phys. Fluids* **7**, 1649–1664.
- PEREGRINE, D. H. 1972 A line source beneath a free surface. *Maths. Res. Center. Univ. of Wisconsin Tech. Summary Rep.* 1248, pp. 1–12.
- PEREGRINE, D. H. 1976 Interaction of water waves and currents. *Adv. Appl. Mech.* **16**, 9–117.
- PEREGRINE, D. H. 1981 The fascination of fluid mechanics. *J. Fluid Mech.* **106**, 59–80.
- PEREGRINE, D. H. & SVENDSEN, I. A. 1978 Spilling breakers, bores and hydraulic jumps. *Proc. 16th Intl Conf. Coastal Engng ASCE* vol. 1, pp. 540–550.
- PHILLIPS, O. M. 1957 On the generation of waves by turbulent wind. *J. Fluid Mech.* **2**, 417–445.
- POGOZELSKI, E. M., KATZ, J. & HUANG, T. T. 1997 The flow structure around a surface piercing strut. *Phys. Fluids* **9**, 1387–1399.
- RAO, N. S. L., SEETHARAMIAH, K. & GANGADHARAI AH, T. 1970 Characteristics of self-aerated flows. *J. Hydr. Engng ASCE* **96**, 331–355.
- RASHIDI, M., HETSRONI, G. & BANERJEE, S. 1992 Wave-turbulence interaction in free-surface channel flows. *Phys. Fluids A* **4**, 2727–2738.
- RAYLEIGH, LORD 1945 *The Theory of Sound*. Reprint of 1894 Edn. Dover.
- REIN, M. 1998 Turbulent open-channel flows: Drop-generation and self-aeration. *J. Hydr. Engng ACSE* **124**, 98–102.
- REYNOLDS, O. 1881 *Brit. Ass. Advan. Sci. Rep.* 524–525.
- ROBERTS, A. J. 1983 Highly nonlinear short-crested water waves. *J. Fluid Mech.* **135**, 301–321.
- ROOD, E. P. 1995 Vorticity interactions with a free surface. In *Fluid Vortices* (ed. S. I. Green). Kluwer.
- SARPKAYA, T. 1996 Vorticity, free-surface, and surfactants. *Ann. Rev. Fluid Mech.* **28**, 88–128.
- SCHÄFFER, H. A., MADSEN, P. A. & DEIGAARD, R. 1993 *Coastal Engng* **20**, 185–202.
- SCOTT, J. C. 1976 The preparation of water for surface-clean fluid mechanics. *J. Fluid Mech.* **69**, 339–351.
- SCOTT, J. C. 1982 Flow beneath a stagnant film on water: the Reynolds ridge. *J. Fluid Mech.* **116**, 283–296.
- SHEN, L., ZHANG, X., YUE, D. K. P. & TRIANTAFYLLOU, G. S. 1999 The surface layer for free-surface turbulent flows. *J. Fluid Mech.* **386**, 167–212.
- SHERIDAN, J., LIN, J. C. & ROCKWELL, D. 1997 Flow past a cylinder close to a free surface. *J. Fluid Mech.* **330**, 1–30.
- SHIKHMURZAEV, Y. D. 1997 Moving contact lines in liquid/liquid/solid systems. *J. Fluid Mech.* **334**, 211–249.
- SHIKHMURZAEV, Y. D. 1998 On cusped interfaces. *J. Fluid Mech.* **359**, 313–328.
- SIMONS, R. R., GRASS, A. J. & KYRIACOU, A. 1988 The influence of currents on wave attenuation. *Proc. 21st Intl Conf. Coastal Engng ASCE* vol. 1, pp. 363–376.
- SVENDSEN, I. A. & MADSEN, P. A. 1984 A turbulent bore on a beach. *J. Fluid Mech.* **148**, 73–96.
- SWEAN, T. F., LEIGHTON, R. I., HANDLER, R. A. & SWEARINGEN, J. D. 1991 Turbulence modeling near the free surface in an open channel flow. *AIAA Paper* 91-0613.
- TEIXEIRA, M. A. C. & BELCHER, S. E. 2000 The initial generation of surface waves by turbulent shear flow. *Preprint*.
- TELES DA SILVA, A. F. & PEREGRINE, D. H. 1988 Steep steady surface waves on water of finite-depth with constant vorticity. *J. Fluid Mech.* **195**, 281–302.
- THORPE, S. A. 1992 Bubble clouds and the dynamics of the upper ocean. *Q. J. R. M. Soc.* **118**, 1–22.
- THORPE, S. A. 1995 Dynamical processes of transfer at the sea surface. *Prog. Oceanogr.* **35**, 315–352.
- THORPE, S. A., BOWYER, P. & WOOLF, D. K. 1992 Some factors affecting the size distributions of oceanic bubbles. *J. Phys. Oceanogr.* **22**, 382–389.
- TSAI, W.-T. 1998 A numerical study of the evolution and structure of a turbulent shear layer under a free surface. *J. Fluid Mech.* **354**, 239–276.

- TSAI, W.-T. & YUE, D. K. P. 1996 Computations of nonlinear free-surfaces flows. *Ann. Rev. Fluid Mech.* **28**, 249–278.
- VOLKART, P. 1980 The mechanism of air-bubble entrainment in self-aerated flows. *Intl J. Multiphase Flow* **6**, 411–423.
- WALKER, D. T. 1997 On the origin of the ‘surface current’ in turbulent free-surface flows. *J. Fluid Mech.* **339**, 275–285.
- WALKER, D. T., CHEN, C.-Y. & WILLMARTH, W. W. 1995 Turbulent structure in free-surface jet flows. *J. Fluid Mech.* **291**, 223–261.
- WALKER, D. T., LEIGHTON, R. I. & GARZANOS, L. O. 1996 Shear-free turbulence near a flat surface. *J. Fluid Mech.* **320**, 19–51.
- WEISSENBORN, P. K. & PUGH, R. J. 1996 Surface tension of aqueous solutions of electrolytes: Relationship with ion hydration, oxygen solubility, and bubble coalescence. *J. Colloid Interface Sci.* **184**, 550–563.
- WILHELMS, S. C. & GULLIVER, J. S. (EDS.) 1991 *Air-Water Mass Transfer*. ASCE.
- YEH, H. 1995 Free surface dynamics. In *Advances in Coastal and Ocean Engineering*, vol. 1 (ed. P. L. F. Liu), pp. 1–75. World Scientific.
- ZAPPA, C. J., ASHER, W. E. & JESSUP, A. T. 2001 Microscale wave breaking and air-water gas transfer. *J. Geophys. Res.* **106**, C5, 9385–9391.